SOUTHWEST CENTER FOR ADVANCED STUDIES
POST OFFICE BOX 30365
DALLAS, TEXAS 75230

DIVISION OF THE
GRADUATE RESEARCH CENTER
OF THE SOUTHWEST

ADAMS 1-1471

GPO PRICE $ _____

CFSTI PRICE(S) $ _____

Hard copy (HC) 1.00

Microfiche (MF) .50

N66-12351 N66-12353

(ACCESSION NUMBER) (THRU)
27 1
(PAGES) (CODE)
CR 67941 29
(NASA CR OR TMX OR AD NUMBER) (CATEGORY)

FACILITY FORM 602

September 8, 1965

Mrs. Winnie M. Morgan
Technical Reports Officer
Grants & Research Contracts Division
Office of Space Science & Applications
NASA
Washington, D. C.

RE: Quarterly Progress Report
Periods covered: April 1-June 30,1965
and July 1 - September 30, 1965
NASr-198

Dear Mrs. Morgan:

Since writing the last report (April 1), balloon flights have been made from India, Australia, and Churchill, Canada. The results from the X-ray astronomy experiment flown from India have been partially reduced, and indicate that there is a source of 20-58 kev X-rays in the constellation Cygnus. A preprint of a paper detailing these results is attached.

The power spectrum and complex demodulation techniques developed earlier for the analysis of the balloon experiments have been applied to the analysis of neutron monitor data in order to study the second harmonic of the cosmic ray anisotropy. Such a harmonic is found, the maximum flux arriving from a direction at right angles to the direction of the interplanetary magnetic field. A preprint of this work is attached.

A comprehensive set of bremsstrahlung X-ray records were obtained during a series of 8 flights from Churchill, Canada. The balloons were hand launched by GRCSW personnel, thereby giving a great deal of flexibility to the programme The data are currently being analysed.

The main part of the Churchill programme, namely, six flights of large experiments by the Skyhook contractor, was not very successful. Only one successful flight was made, while two further launch attempts failed.

Preparations are being made to fly the X-ray spark chamber experiment, and a second-generation X-ray astronomy experiment from Palestine, Texas, during September, 1965.

Yours sincerely,

K. G. McCracken

K. G. McCracken

KGMcC:abj
attachments (2)(preprints)
cc: Messrs. D. W. Canham and J. S. Robottom

THE SEMI-DIURNAL ANISOTROPY OF THE COSMIC RADIATION

[redacted]

by

J. G. Ables, K. G. McCracken, and U. R. Rao

Southwest Center for Advanced Studies
Dallas, Texas

To be presented at

The 9th International Conference on Cosmic Rays
London, England
September 6-17, 1965

ACKNOWLEDGEMENT - This research has been supported by the National Aeronautics and Space Administration under contract NASr-198 and by the Air Force Cambridge Research Laboratories under contract AF19(628)-5028.

THE SEMI-DIURNAL ANISOTROPY OF THE COSMIC RADIATION

by

J. G. Ables, K. G. McCracken, and U. R. Rao
Southwest Center for Advanced Studies
P. O. Box 30365
Dallas, Texas

N66-12352

ABSTRACT

12352

Using data from 14 different neutron monitors, the semi-diurnal anisotropy of the cosmic radiation during the period 1953-1965 has been investigated. Numerical filter techniques, consisting of numerical heterodyne filtration followed by phase and amplitude demodulation (complex demodulation) has been employed. This process reduces to ordinary harmonic analysis as a special case. The effective filter response function for harmonic analysis is compared with the more desirable response functions employed in this investigation.

Phase and amplitude distribution histograms for each station and year have been constructed which, when fully corrected for the effects of geomagnetic bending of primary trajectories, indicate a consistent semi-diurnal anisotropy having an amplitude of approximately 0.1% and maxima along a line 60° west of the earth-sun line. A study of the energy dependence of this anisotropy has been made which, though not conclusive, indicates that the anisotropy may be energy dependent.

1. INTRODUCTION

In addition to the well known diurnal variation in the cosmic ray flux, observers have long noted a statistically significant 12 hour, semi-diurnal, periodicity. The existence of such a periodicity is not surprising, since the interplanetary magnetic field exhibits a relatively fixed mean direction (Ness, 1964), and therefore defines a bifurcated reference direction in space, particle motions (both guiding centre, and diffusion) differing strongly for motion parallel to, and normal to the field. The resultant bifurcation of the cosmic ray anisotropy would be observed on the earth as a semi-diurnal periodicity.

The experimentally observed semi-diurnal variations are of amplitude $\sim$ 0.1% for neutron monitors, and hence tend to be masked by statistical noise. While data employing crossed meson telescopes [eg, Rao and Sarabhai (1961), Ahluwalia (1962)] provide clear-cut evidence for a semi-diurnal variation of extra-terrestrial origin, the neutron data obtained by a world wide

net of neutron monitors in 1957-58 was not consistent with a semi-diurnal anisotropy.

In this paper, a thorough study has been made of the semi-diurnal variation using modern numerical filter techniques, since these offer some improvement in the detection of the small signal (the semi-diurnal variation) in the presence of noise (statistical fluctuations). The analysis employs data from the large neutron monitors described by Hatton and Carmichael (1964) thereby producing further improvement in the signal to noise ratio.

2. THEORY

In order to simplify the work we shall, for the following discussion, assume that the data are continuous and extend throughout all time. In fact, of course, the data are discrete and limited to a finite time interval. The extension of the results to the discrete case is,however, straightforward, although tedious, and some care must be exercised.

Let the data be a function of time of the form

$$f(t) = A(t)\cos[\omega_0 t + \Phi(t)] + N(t) \qquad \ldots (2.1)$$

where the cosine term represents the signal and N(t) represents all other components of the data record which we shall call the <u>noise</u>. From the data, we desire to extract, with maximum accuracy, the information carried by the functions A(t) and Φ(t). Consider the properties of the integral transform of f(t) given by

$$C(t,\omega_0) = \int_{-\infty}^{\infty} D(t'-t) f(t') e^{i\omega_0 t'} dt' \qquad \ldots (2.2)$$

where D(t) is an even function satisfying the condition

$$\int_{-\infty}^{\infty} D(t)\, dt = 1 . \qquad \ldots (2.3)$$

We may treat this transformation as a two step process.

<u>Multiplication of the signal function by</u> $e^{i\omega_0 t}$. This is a heterodyning or spectrum shifting operation. If f(t) has an autocorrelation function R(τ), then the power spectral density function (power spectrum) of f(t) is given by

$$S(\omega) = \int_{-\infty}^{\infty} R(\tau) e^{-i\omega\tau} d\tau \qquad \ldots (2.4)$$

which is formally equivalent to

$$S(\omega) = \lim_{T\to\infty} \frac{1}{2T} \left| \int_{-T}^{T} f(t) e^{-i\omega t} dt \right|^2 . \qquad \ldots (2.5)$$

Hence, the power spectrum of $f(t)e^{i\omega_0 t}$ is given by

$$S'(\omega) = \lim_{T\to\infty} \frac{1}{2T} \left| \int_{-T}^{T} f(t) e^{-i(\omega-\omega_0)t} dt \right|^2 . \qquad \ldots (2.6)$$

so that

$$S'(\omega) = S(\omega - \omega_0) \, . \qquad \ldots (2.7)$$

This implies that each spectral component of the signal function is shifted in the frequency domain by an amount ω_0. Thus, those spectral components originally in the neighborhood of ω_0 will now lie in the neighborhood of zero frequency.

<u>Convolution of the heterodyned signal with the weighting function D(t)</u>. Let the Fourier integral transform of D(t) be

$$Y(\omega) = \int_{-\infty}^{\infty} D(t) e^{-i\omega t} dt \, . \qquad \ldots (2.8)$$

Then, since convolution in the time domain is equivalent to multiplication of spectra (filtering) in the frequency domain, the power spectrum of the heterodyned signal function convolved with D(t) is simply

$$S''(\omega) = |Y(\omega)|^2 S'(\omega) = |Y(\omega)|^2 S(\omega - \omega_0) \, . \qquad \ldots (2.9)$$

Now if D(t) is chosen so that $Y(\omega)$ is non-zero only in some small region about zero frequency, then it is clear that the only spectral components of f(t) which will contribute to $C(t, \omega_0)$ will be those lying in an equivalent small frequency band about ω_0. By the condition given in (2.3), $|Y(0)|^2 = 1$ so that the weighting given to components of frequency ≈ 0 is unity. Also, since we chose D(t) to be an even function, $Y(\omega)$ is real and hence no phase shift is introduced by the filtering.

The usefulness of this transform (2.2) becomes apparent when it is applied to a signal similar to that given in (2.1). In this case $C(t, \omega_0)$ is

$$\begin{aligned} C(t, \omega_0) = {} & \overline{A(t)\cos[\omega_0 t + \phi(t)]\cos(\omega_0 t)} \\ & + i\,\overline{A(t)\cos[\omega_0 t + \phi(t)]\sin(\omega_0 t)} + C_N \\ = {} & \tfrac{1}{2}\,\overline{A(t)\cos[\phi(t)]} + \tfrac{1}{2}\,\overline{A(t)\cos[2\omega_0 t + \phi(t)]} \\ & + \tfrac{i}{2}\,\overline{A(t)\sin[-\phi(t)]} + \tfrac{i}{2}\,\overline{A(t)\sin[2\omega_0 t + \phi(t)]} \\ & + C_N \, . \end{aligned} \qquad \ldots (2.10)$$

The bar represents the filtering operation (convolution with D(t)) and C_N is the integral transform of N(t). If, as suggested before, $|Y(\omega)|^2$ is non-zero only for some small frequency band about zero frequency, then the second and fourth terms of the last expression above are zero due to the $2\omega_0 t$ terms in the argument of the sine and cosine factors. Also, if N(t) is a wideband noise whose power per unit frequency interval in the neighborhood of ω_0 is small compared with the power of $A(t)\cos[\omega_0 t + \phi(t)]$ in this neighborhood, then we

may neglect C_n as a first approximation. For $\phi(t)$ a slowly varying function of time, the first and third terms of (2.10) have frequency ≈ 0 so that the bar may be removed since $|Y(0)|^2 = 1$. This yields

$$C(t,\omega_0) = \frac{1}{2} A(t)\cos[\phi(t)] - \frac{i}{2} A(t)\sin[\phi(t)] = \frac{A(t)}{2} e^{-i\phi(t)} \quad \ldots \quad (2.11)$$

So that, finally, we have

$$A(t) = 2|C(t,\omega_0)|$$
$$\phi(t) = -\arg C(t,\omega_0). \quad \ldots \quad (2.12)$$

It is apparent that the transform of (2.2) may be used as a device for extracting the phase and amplitude in the presence of wideband noise. Furthermore, with a knowledge of the power spectrum of the signal of interest and of the interfering noise it is possible to tailor the filter response function $|Y(\omega)|^2$ to maximize the contribution of the desired signal components to $C(t,\omega_0)$ while minimizing the noise contribution. Figure 1 shows a typical neutron monitor power spectrum. A significant spectral peak appears at 2 cycles per day (cpd) indicating the presence of a semi-diurnal variation with amplitude considerably greater than the r.m.s. noise amplitude in the neighborhood of 2 cpd. The relative narrowness of the peak (~0.1 cpd) points out the advantage to be realized with narrow band filtering.

For the same purpose, it is common to express the signal function, f(t) as a Fourier series on some finite interval of duration T centered on time t_0. This gives

$$f(t) = \sum_{-\infty}^{\infty} C_n(t_0,\omega_n) e^{i\omega_n t} \qquad t_0 - \frac{T}{2} \leq t \leq t_0 + \frac{T}{2} \quad \ldots \quad (2.13)$$

$$C_n(t_0,\omega_n) = \frac{1}{T}\int_{t_0-T/2}^{t_0+T/2} f(t) e^{-i\omega_n t}\, dt \quad \ldots \quad (2.14)$$

The expression for the complex Fourier coefficient, C_n given above is identical to the transform given in (2.2) if D(t) is taken as

$$D_0(t) = \frac{1}{T} \qquad t_0 - \frac{T}{2} \leq t \leq t_0 + \frac{T}{2} \quad \ldots \quad (2.15)$$
$$D_0(t) = 0 \qquad \text{elsewhere}$$

thus demonstrating that classical harmonic analysis is a special case of the more general process described by (2.2). Such processes have been called <u>complex demodulation</u> since they represent an inverse to the process of complex modulation, that is, simultaneous amplitude and phase modulation.

<u>Filter response functions</u>. Desirable filter response functions have essentially unity response within the frequency interval of interest and essentially zero response elsewhere. Three filter functions used were of the form

$$D(t) = N e^{-\beta t^2} \frac{\sin \alpha t}{t} \quad \ldots \quad (2.16)$$

The parameter α determines the bandwidth of the filter and β is chosen to damp the impulse response to prevent overshoot and ringing. N is a normalization constant chosen so that condition (2.3) is satisfied. A fourth filter function of the form of (2.15) was also employed to produce a standard harmonic analysis for comparison. The filter functions are characterized by their rise times (time required for transition from 10% to 90% of full response when activated by the unit step function) which is the reciprocal of their effective bandwidths. It may be noted that $D_0(t)$ (2.15) has a response function of the form

$$|Y_0(\omega)|^2 = K \frac{\sin^2\left(\frac{\omega T}{2}\right)}{(\omega T/2)^2} \qquad \ldots (2.17)$$

which exhibits a widespread multi-lobed structure that is less desirable in most cases than a filter with a single rectangular-shaped peak. Figure 2 compares the response functions of harmonic analysis with the responses which may be achieved by means of convolution with weighting functions of the type of (2.16). Note that complete elimination of the far-ranging side lobes of ordinary harmonic analysis may be obtained at no sacrifice of response speed (rise time).

Reduction of the data. Data from the world-wide net of neutron monitoring stations was selected by a criterion of self-consistency in the manner described by Rao et al (1963). For a station meeting this criterion all data were accepted. For the years 1953-1956 little data are available and the selection criterion was relaxed. The data from all stations were demodulated using filters of one, five, and fifteen day rise times. For each station and year histograms were constructed showing the distribution of the time of maximum and amplitude. A smooth curve was fitted to the phase histograms and the position of the peak of this curve was taken as an estimate of the most probable time of maximum. Times of maximum so determined were corrected to asymptotic time (local time of the asymptotic cone of acceptance) (Rao et al, 1963). Parameters of the asymptotic cones of acceptance were taken from McCracken et al (1965). The anisotropy was assumed to be energy independent in these calculations.

3. RESULTS

The histograms of the semi-diurnal time of maximum using the 15-day rise time filter show very significant peaks for all stations and years (Figure 3). Similar histograms drawn from the results of daily harmonic analysis show no such peaks for I.G.Y. monitors and only small peaks for even the new NM-64 supermonitors.

The times of maximum of the various stations, when stated in local times, have a wide dispersion, no correlation being noticed between these times and the phase of the station semi-diurnal barometric pressure waves reported by Katzman and Venkatesan (1960). When expressed in asymptotic time, however, excellent inter-station agreement is found for the years 1962-1965, the standard error being as small as 8 degrees for 1963 and only slightly larger for other years. For the period 1957-1961 the dispersion increases, but

reasonable agreement is retained with only one or two stations being exceptional cases. Prior to 1957 the number of reporting stations is too small to produce definite results, however, these data are included in Figure 4 which summarizes the results of the determination of the semi-diurnal time of maximum for the entire survey. The steadily decreasing scatter among individual stations for later years is more reasonably attributed to the constant improvement of monitoring facilities rather than to a basic change in the cosmic ray variation. Amplitude distribution histograms (Figure 5) indicate a most probable amplitude of approximately 0.1%.

The semi-diurnal phase is remarkably constant for the solar cycle 1955-1965 indicating a primary bidirectional anisotropy having maximum flux along a line 60°west of the earth-sun line (Figure 6), a direction which is essentially perpendicular to the interplanetary magnetic field reported by Ness and Wilcox (1964). A study of the inter-station variance in phase as a function of the assumed variational rigidity spectrum shows some preference for a power law spectrum with a positive exponent of 0.5 . However, the statistical errors for this determination are large and an energy independent variational spectrum for the semi-diurnal anisotropy can not be ruled out.

ACKNOWLEDGEMENT

We wish to express our gratitude to the many investigators who provided the data used herein.

REFERENCES

Ahluwalia, H. S., 1962, Proc. Phys. Soc., 80, 472
Hatton, C. and Carmichael, H., 1964, Can. J. Phys. 42, 2443
Katzman, J. and Venkatesan, D., 1960 Can. J. Phys. 38, 1011
McCracken, K. G., Rao, U. R., Fowler, B. C., Shea, M. A. and Smart, D., 1965, I.Q.S.Y. Instruction Manual # 10
Ness, N. and Wilcox, J., 1964, Phys. Rev. Lttrs. 13 ,461
Rao, U. R. and Sarabhai, V., 1961, Prpc. Roy. Soc. 263, 101
Rao, U. R., McCracken, K. G. and Venkatesan, D., 1963, J. Geophys. Res. 68, 345

CAPTIONS FOR FIGURES

Fig. 1 A neutron monitor data power spectrum showing the presence of narrow-band periodic variation at 1 cpd and 2 cpd

Fig 2 A comparison of the effective filter response of harmonic analysis with the more desirable filter responses used in this study

Fig. 3 Typical distribution histograms of the first time of maximum of the semi-diurnal variation obtained with a narrow-band filter.

Fig. 4 The inter-station dispersion and yearly mean value of the semi-diurnal phase for the years 1953-65.

Fig. 5 Typical distribution histrograms of the semi-diurnal amplitude obtained with a narrow-band filter.

Fig. 6 24-hour dials showing the relationship between the semi-diurnal first time of maximum and the earth-sun line

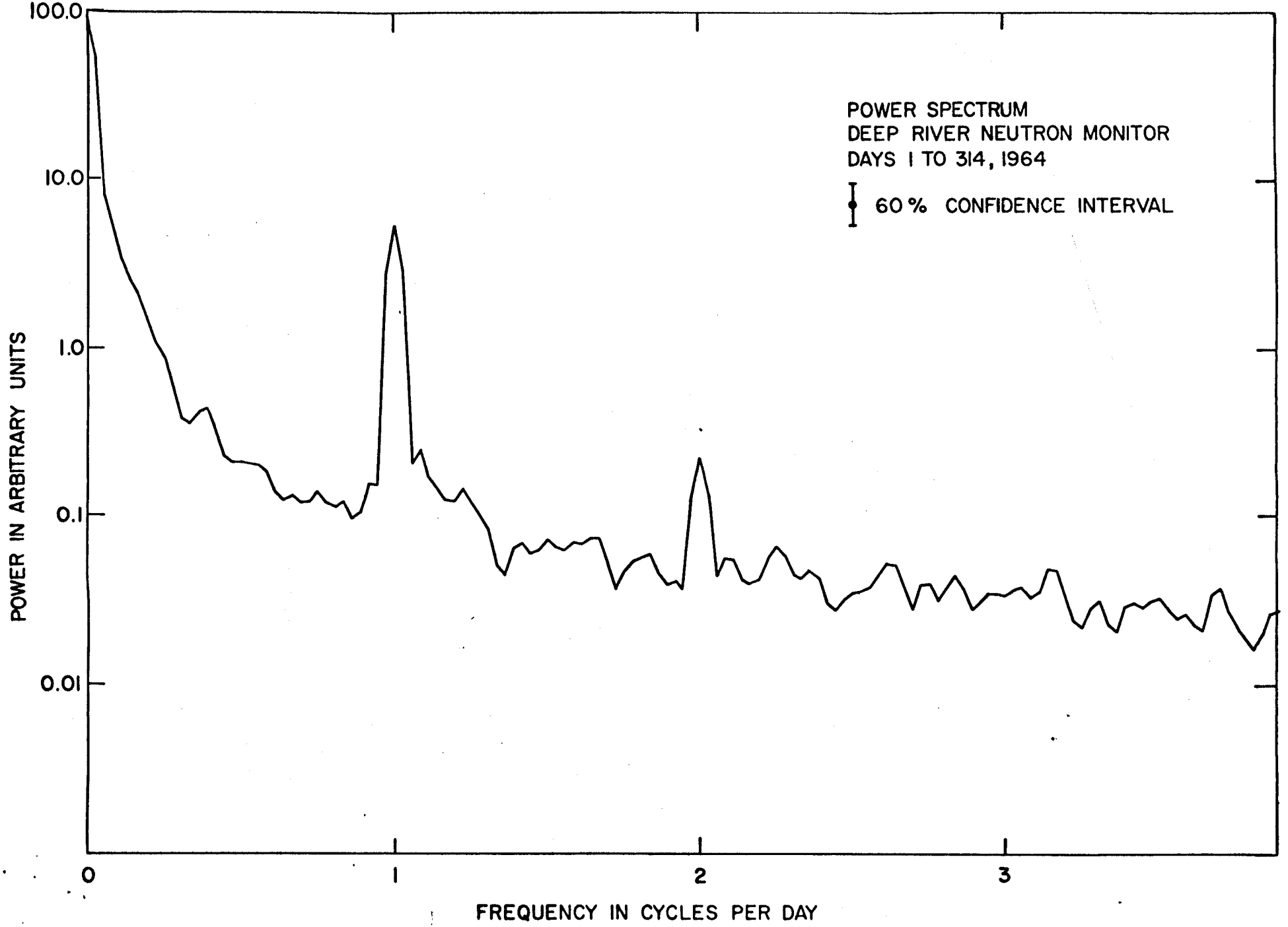
POWER SPECTRUM
DEEP RIVER NEUTRON MONITOR
DAYS 1 TO 314, 1964
60 % CONFIDENCE INTERVAL
100.0
10.0
1.0
0.1
0.01
POWER IN ARBITRARY UNITS
0
1
2
3
FREQUENCY IN CYCLES PER DAY

FIG. 1

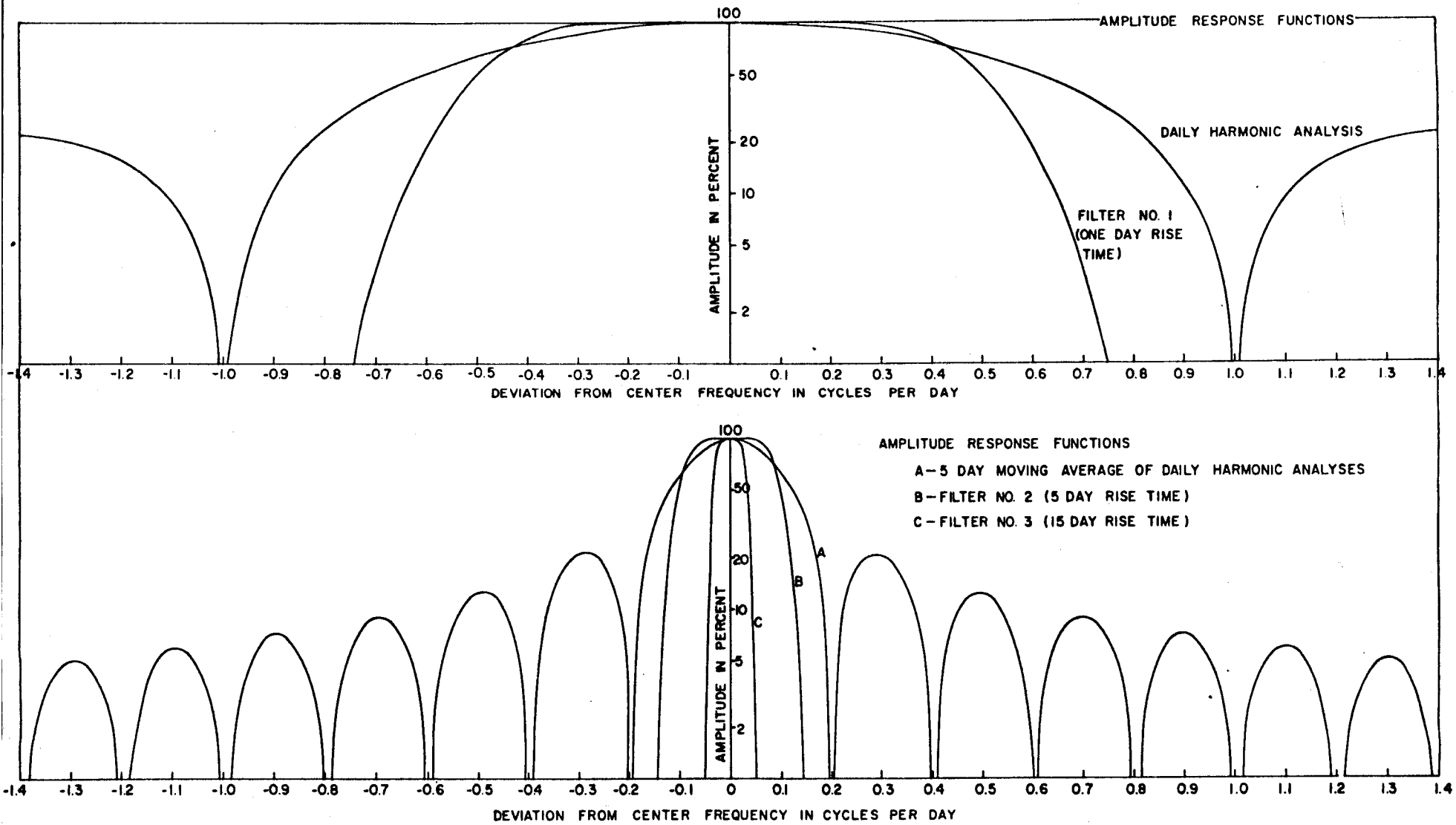
AMPLITUDE RESPONSE FUNCTIONS
DAILY HARMONIC ANALYSIS
FILTER NO. 1 (ONE DAY RISE TIME)
AMPLITUDE IN PERCENT
100
50
20
10
5
2
-1.4 -1.3 -1.2 -1.1 -1.0 -0.9 -0.8 -0.7 -0.6 -0.5 -0.4 -0.3 -0.2 -0.1 0.1 0.2 0.3 0.4 0.5 0.6 0.7 0.8 0.9 1.0 1.1 1.2 1.3 1.4
DEVIATION FROM CENTER FREQUENCY IN CYCLES PER DAY
AMPLITUDE RESPONSE FUNCTIONS
A – 5 DAY MOVING AVERAGE OF DAILY HARMONIC ANALYSES
B – FILTER NO. 2 (5 DAY RISE TIME)
C – FILTER NO. 3 (15 DAY RISE TIME)
A
B
C
AMPLITUDE IN PERCENT
100
50
20
10
5
2
-1.4 -1.3 -1.2 -1.1 -1.0 -0.9 -0.8 -0.7 -0.6 -0.5 -0.4 -0.3 -0.2 -0.1 0 0.1 0.2 0.3 0.4 0.5 0.6 0.7 0.8 0.9 1.0 1.1 1.2 1.3 1.4
DEVIATION FROM CENTER FREQUENCY IN CYCLES PER DAY

FIG. 2

HISTOGRAM OF ϕ_2 USING 15 DAY RISE TIME FILTER FOR 1964

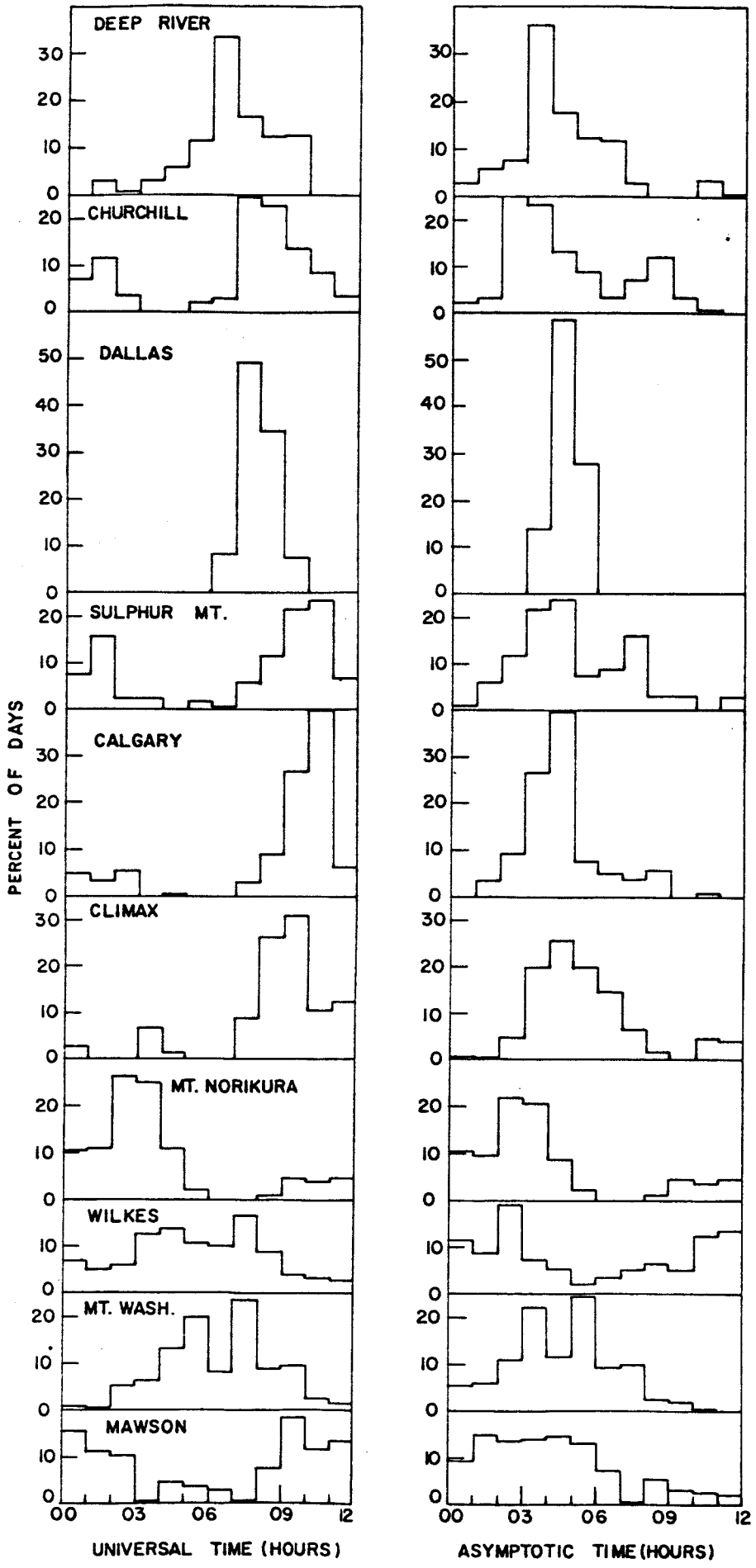

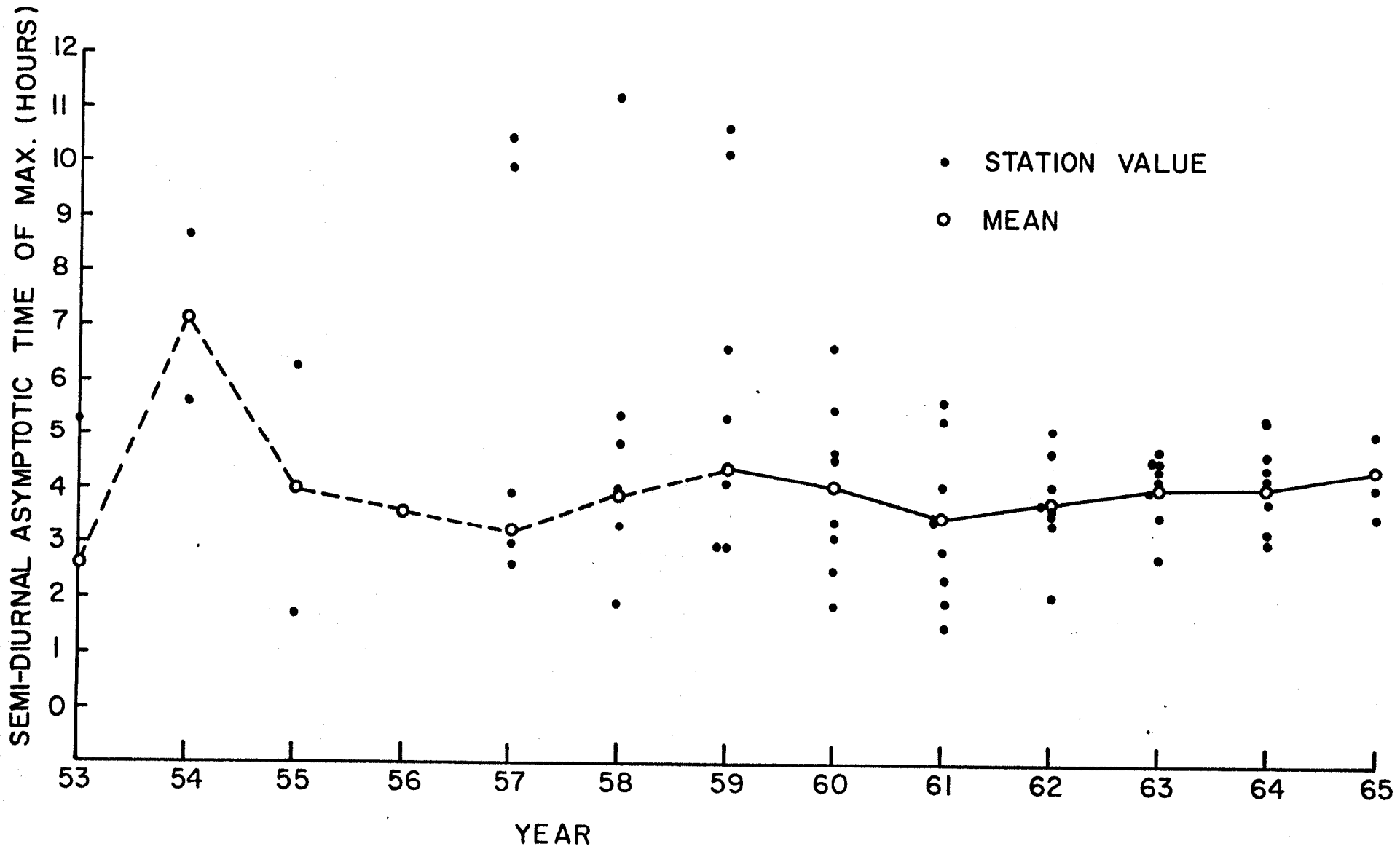
SEMI-DIURNAL ASYMPTOTIC TIME OF MAX. (HOURS)
12
11
10
9
8
7
6
5
4
3
2
1
0
STATION VALUE
MEAN
53
54
55
56
57
58
59
60
61
62
63
64
65
YEAR

FIG. 4

HISTOGRAM OF R_2 USING 15 DAY RISE TIME FILTER FOR 1964

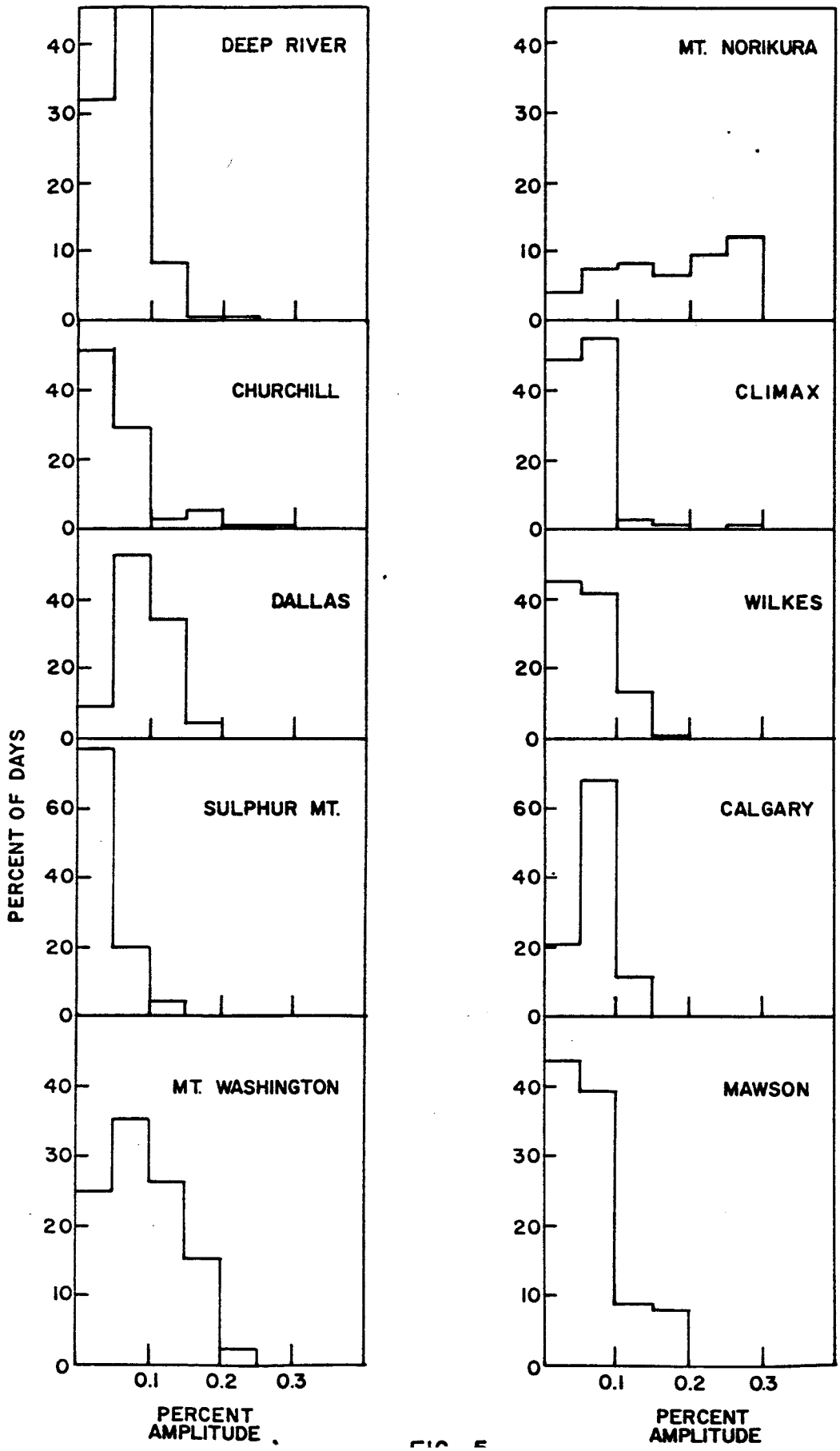

FIG. 5

DIRECTION OF SEMI-DIURNAL ANISOTROPY

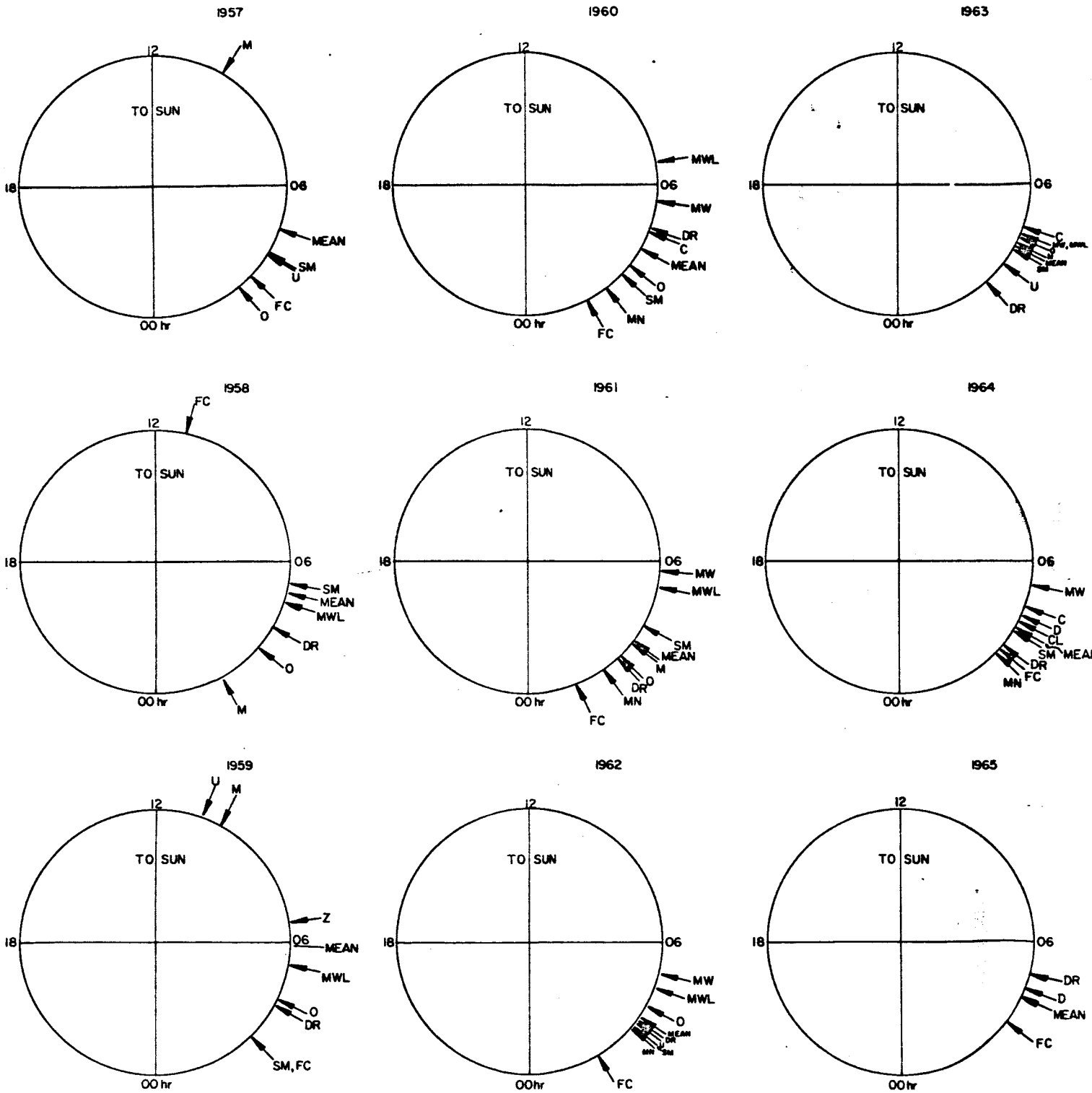

FIG. 6

A CELESTIAL SOURCE OF X-RAYS IN THE ENERGY RANGE 20 TO 58 KEV

N66-12353

by

K. G. McCracken

Southwest Center for Advanced Studies
Dallas, Texas

To be presented at

The 9th International Conference on Cosmic Rays
London , England
September 6-17, 1965

ACKNOWLEDGEMENT - This research has been supported by the National Aeronautics and Space Administration under grants NASr-198 and NsG-269-82.

A CELESTIAL SOURCE OF X-RAYS IN THE ENERGY RANGE 20 TO 58 KEV

by

K. G. McCracken
Southwest Center for Advanced Studies
P. O. Box 30365
Dallas, Texas

ABSTRACT

12353

An experiment designed to search for celestial sources of X-rays in the energy range 20-58 kev is described.

A source of X-rays has been observed in the constellation Cygnus, and a tentative identification with Cygnus XR-1 is made. The X-ray, and radio data indicate that the spectrum of the Cyg XR-1 source is significantly different from that of the X-ray/radio emitter Taurus A.

Author

1. INTRODUCTION

A series of balloon flights has been made to search for celestial sources of 0.3 to 0.8 Å X-rays. Two flights were made from Hyderabad, India (17°25'N, 78°35'E), and to date, one from Mildura, Australia (34°13'S,142°05'E). The total coverage, to date, is summarised in Figure 1, where the portions of the celestial sphere scanned during any flight are defined as those which were within 40° of the zenith at any time during the period a balloon was at altitude. This paper presents preliminary results of the Indian flights.

2. INSTRUMENTATION

Figures 2 and 3 summarise the physical arrangement of the detector, and the block diagram of the electronics. The basic detector is a thick (1/2 inch) NaI (Tl) scintillator, of diameter 7 inches, viewed by a 7-inch photomultiplier. The cone of acceptance of the detector is defined by a set of 1/32 inch brass plates, which present a minimum absorption of x 9 for any photon in the energy range 20-58 kev which passes through them. For most paths, the attenuation is greater by a factor of ten or more, and hence the detector has a well defined "fan beam" cone of acceptance. The effective cross-section of the device for the detection of X-rays is illustrated in Figure 2B.

The photomultiplier-crystal combination was observed to have a FWHM line width of 42% for the 30 kev X-rays of Ba^{133}. In the flight equipment, the

photomultiplier pulses were analysed by a pulse height analyser providing five contiguous differential channels between 20 and 58 kev, and an integral channel of $>$ 58 kev.

The complete balloon experiment consisted of two similar X-ray detectors of diameters 7 inches and 5 inches and a charged particle detector. The experiment was connected to the balloon via a "line twister" which caused the experimental package to rotate with a period of 11.2 minutes. The various supporting cables, and the method of attachment of the parachute, were designed to minimise torsional oscillations of the experiment. The experiment was suspended such that the viewing axes of the X-ray detectors made an angle of 22° with the vertical, the fan beam passing through the zenith. There was approximately 200 mg cm^{-2} of matter (polyurethane) above the X-ray detectors.

A Schoenstedt flux-gate magnetometer provided azimuth information, as indicated in Figure 3. The average aximuth and counting rate data were determined every 10.50 seconds throughout the flights. The results presented here are confined to those obtained by the large (7 inch diameter) X-ray detector.

3. RESULTS

Two successful flights, Hyd-2 and Hyd-3, were made on 2 April 1965 and 8 April 1965, respectively. In both flights, the balloons floated at a constant altitude of 4.5 g cm^{-2}.

Figure 4 presents the 26-45 kev X-ray counting rates observed between 0830 and 1000 IST and 1000 to 1130 IST on April 2, 1965, plotted as a function of geomagnetic azimuth of viewing. In the lower curve, a well defined peak is centred on an azimuth of 34°W. The azimuths of both Cygnus A and XR-1 (Bowyer et al, 1965) at this time are indicated. At this time, the mean position of Cygnus XR-1 was 30° from the zenith; figure 2 indicates that the azimuthal variation of counting rate based on the assumption of a point source of X-rays at this zenith angle is a triangular wave of FWHM 36°. The similarity of the observed counting rate and the theoretical curve suggests that the peak in Figure 4 is due to a flux of 26 to 45 kev X-rays from the general vicinity of Cygnus A or XR-1.

Comparing the two curves in Figure 4, it can be seen that the peak in the curve corresponding to the period 1000-1130 IST is less pronounced than that for the period 0830-1000 and that it is shifted towards the west. Comparing the excess fluxes under the peaks, we find the flux at the later time to be 0.68 ± 0.12 of that at the earlier time, while the mean position of the peak has shifted 16° to the west. For an assumed X-ray source in the direction of Cygnus XR-1 the mean atmospheric thickness differs between the two periods by 0.9 g cm^{-2}, and the average attenuation factor for such a thickness of air for a flat spectrum in the range 26-45 kev is 0.75; the attenuation factor approaching a limiting value of 0.65 as the spectrum steepens. The diurnal rotation of the earth caused the average azimuth of Cygnus XR-1 to move 11° to the west between the times noted above. The quantitative agreement between the observed, and predicted attenuation and the westward shift of the peak supports

the hypothesis that the peaks are due to an X-ray flux from the general direction of Cygnus.

In Figure 5 the data from each of the six pulse height analyser channels is displayed as a function of azimuth for the period 0830-1000 IST. The absence of a peak in channel 6 ($>$58 kev) and the smaller peak in channel 5 (45-58 kev) are all consistent with an extra-terrestrial source of X-rays. From Figure 5, and a similar figure for the period 1000-1130 IST, the manner in which the peak varies with time was determined, being tabulated in Table 1. The selective attenuation of the lower energy channels as the thickness of absorber increases is consistent both qualitatively and quantitatively with the hypothesis that the peak is due to an extra-terrestrial point source of X-rays.

TABLE 1.

The reduction in the flux in the peak at azimuth 34° between the period 0830-1000 IST and 1000-1130 IST. The flux in the latter period is expressed as a fraction of that in the former.

Energy Range (kev)	20-26	26-29	29-34	34-45	45-58
Fraction	0.0	0.16	0.78	0.69	0.91

A preliminary calculation has indicated that the data are consistent with a differential number (of photons) spectrum which varies as E^{-2}, where E is the photon energy. At this time, however, a spectrum varying as E^{-3} is not precluded. From the data in Figure 5, a preliminary estimate of the energy flux has been made, it being found to be 8×10^{-31} watts $m^{-2}(cps)^{-1}$ in the vicinity of 40 kev.

Bowyer et al (1965) observing in the wavelength range 3 to 8 Å have identified two X-ray sources Cyg XR-1 (RA = 19h53m, Dec = +34.6°) and Cyg XR-2 (RA=21h43m, Dec =+38.8°) in the constellation of Cygnus. Their measurements suggest that Cyg XR-1 is the second brightest X-ray source in the sky, and since the data presented herein are consistent with a source in the direction of Cygnus XR-1, we suggest that the source seen by the balloon detector is Cygnus XR-1. The NRL data (Bowyer et al), and the current balloon data lead to the crude spectrum summarised in Figure 6. While it is tempting to associate the X-ray emission with Cygnus A, the brightest radio source in the sky, Bowyer et al have stated that their observations indicate otherwise.

The radio-observations of Piddington and Trent (1956) in the direction of Cygnus XR-1 indicate an antenna temperature of 20°K at 600 mc/sec. Since

the radio isophotes do not show any features in the vicinity which could be associated with emission from Cyg XR-1, we assume that the energy flux from Cyg XR-1 is less than a tenth of the general background from RA=19h53m; Dec = +34.6°. This upper limit to the radio flux from Cyg XR-1 is shown in Figure 6.

The data for Taurus A, as summarised by Clark (1965) , are superposed on Figure 6. It can be seen that the Cygnus spectrum is significantly different from that of the Taurus source at the low fequency end of the spectrum, while the spectral form, and energy fluxes, are similar in the X-ray range.

ACKNOWLEDGEMENT

The India balloon expedition was coordinated and implemented by the National Science Foundation and the National Center for Atmospheric Research, under the able guidance of Dr. B. Stiller and Messrs. R. Kubara and T. Pappas. The assistance of Mr. J. Corwin and Miss M. Steinbock in the construction of the equipment and the data analysis, respectively, is gratefully acknowledged.

REFERENCES

Bowyer, S., Bynam, E. T., Chubb, T. A., and Freidman, H., 1965, Science 147, 394-398

Clark, G. W., 1965, Phys. Rev. Lttrs 14 , 91-94.

Piddington, J. H., and Trent, G. H., 1956, Austral. J. Phys. 9, 481-493.

FIGURE CAPTIONS

Fig. 1 The regions of the celestial sphere scanned during the Indian, and one Australian flight.

Fig. 2a Illustrating the physical arrangement of the mechanical collimator in front of the scintillator-photomultiplier combination.

Fig. 2b The detector cross section as a function of viewing angle.

Fig. 3 A simplified block diagram of the balloon-bourne X-ray detector, and its ground station.

Fig. 4 The counting rate of X-rays in the energy range 20-45 kev as a function of geomagnetic azimuth, measured westward from geomagnetic north.

Fig. 5 The counting rates of the six pulse height channels as a function of geomagnetic azimuth.

Fig. 6 The spectrum of the Cygnus XR-1 source. The spectrum reported by Clark for Taurus A is superposed.

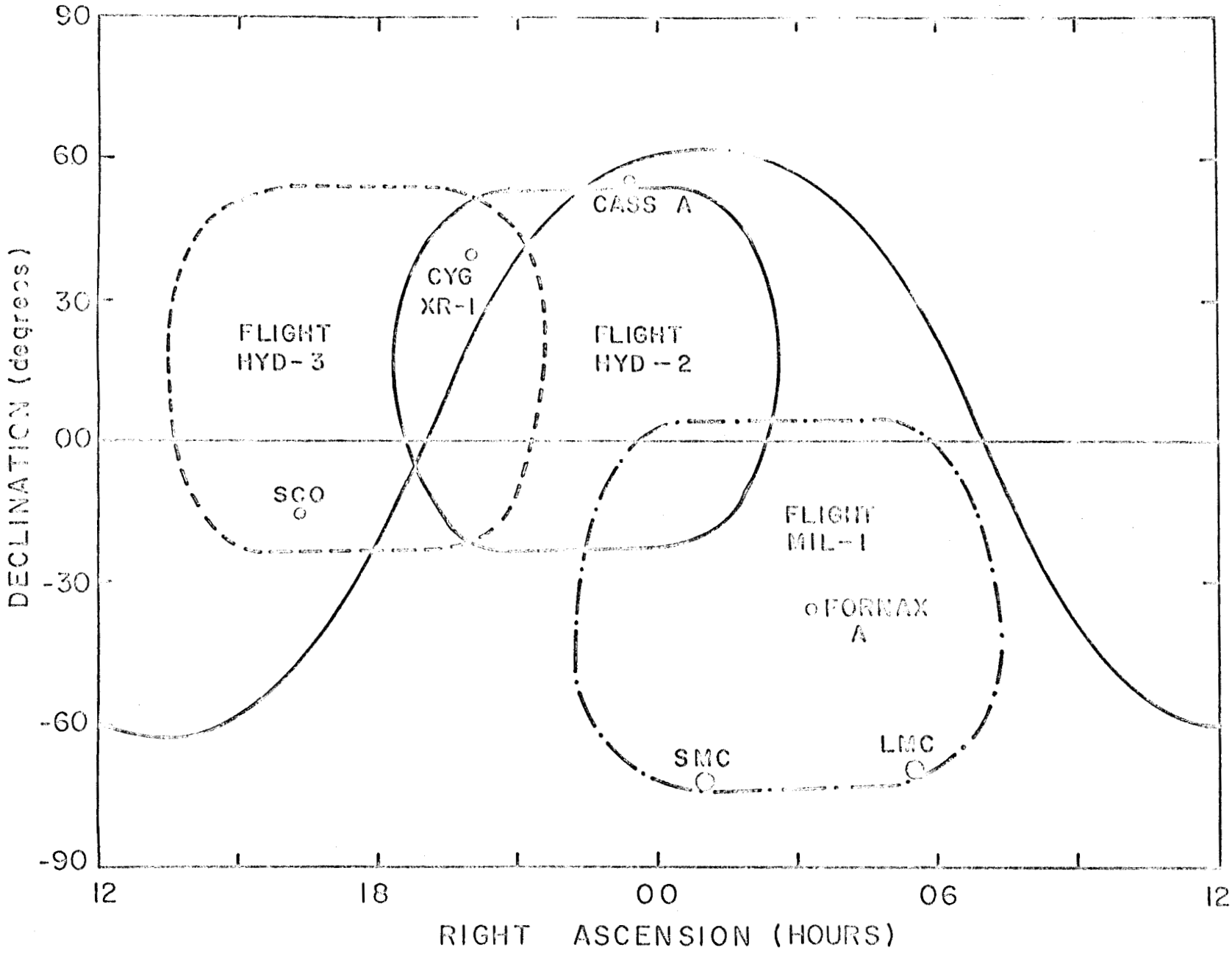
90
60
30
00
-30
-60
-90
DECLINATION (degrees)
12
18
00
06
12
RIGHT ASCENSION (HOURS)
CASS A
CYG
XR-1
FLIGHT
HYD-3
FLIGHT
HYD--2
SCO
FLIGHT
MIL-1
FORNAX
A
SMC
LMC

FIG. 1

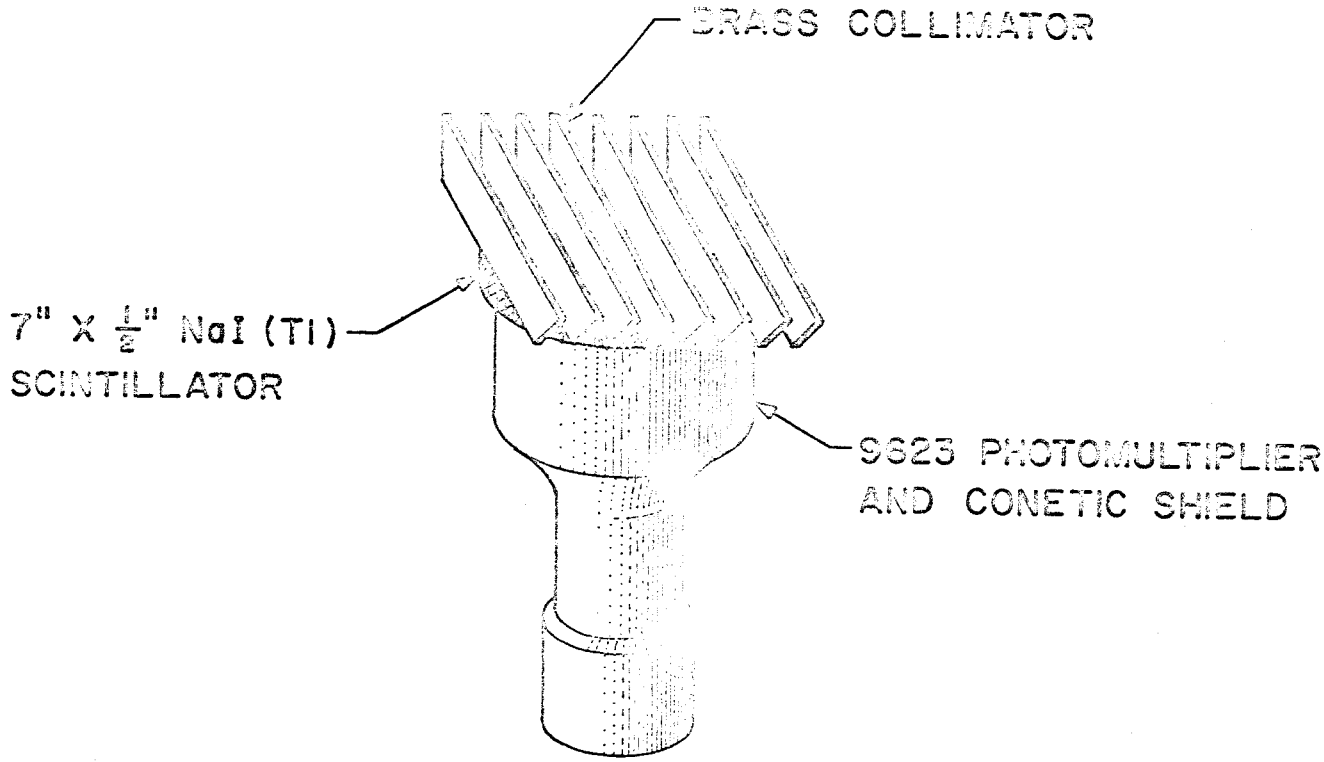
BRASS COLLIMATOR
7" X 1/2" NaI (Tl)
SCINTILLATOR
9623 PHOTOMULTIPLIER
AND CONETIC SHIELD

FIG. 2A

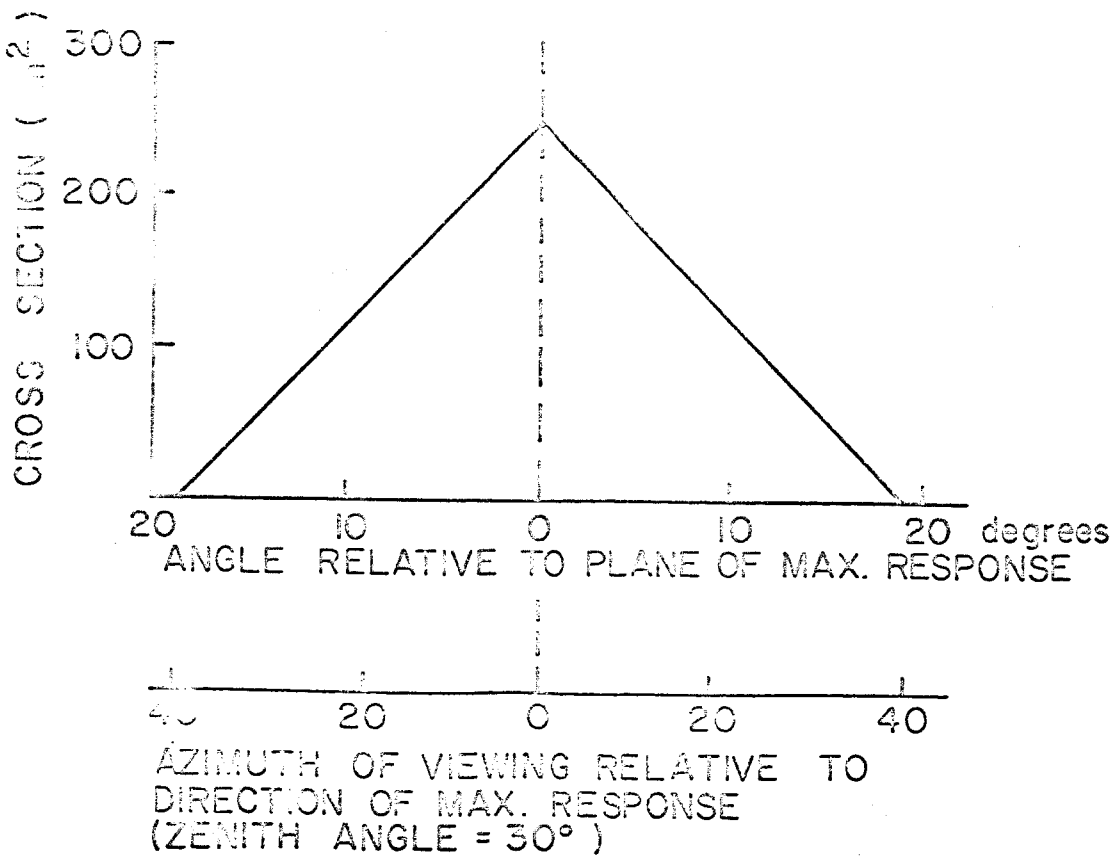
CROSS SECTION (m2)
300
200
100
20
10
0
10
20 degrees
ANGLE RELATIVE TO PLANE OF MAX. RESPONSE
20
0
20
40
AZIMUTH OF VIEWING RELATIVE TO
DIRECTION OF MAX. RESPONSE
(ZENITH ANGLE = 30°)

BALLOON EQUIPMENT

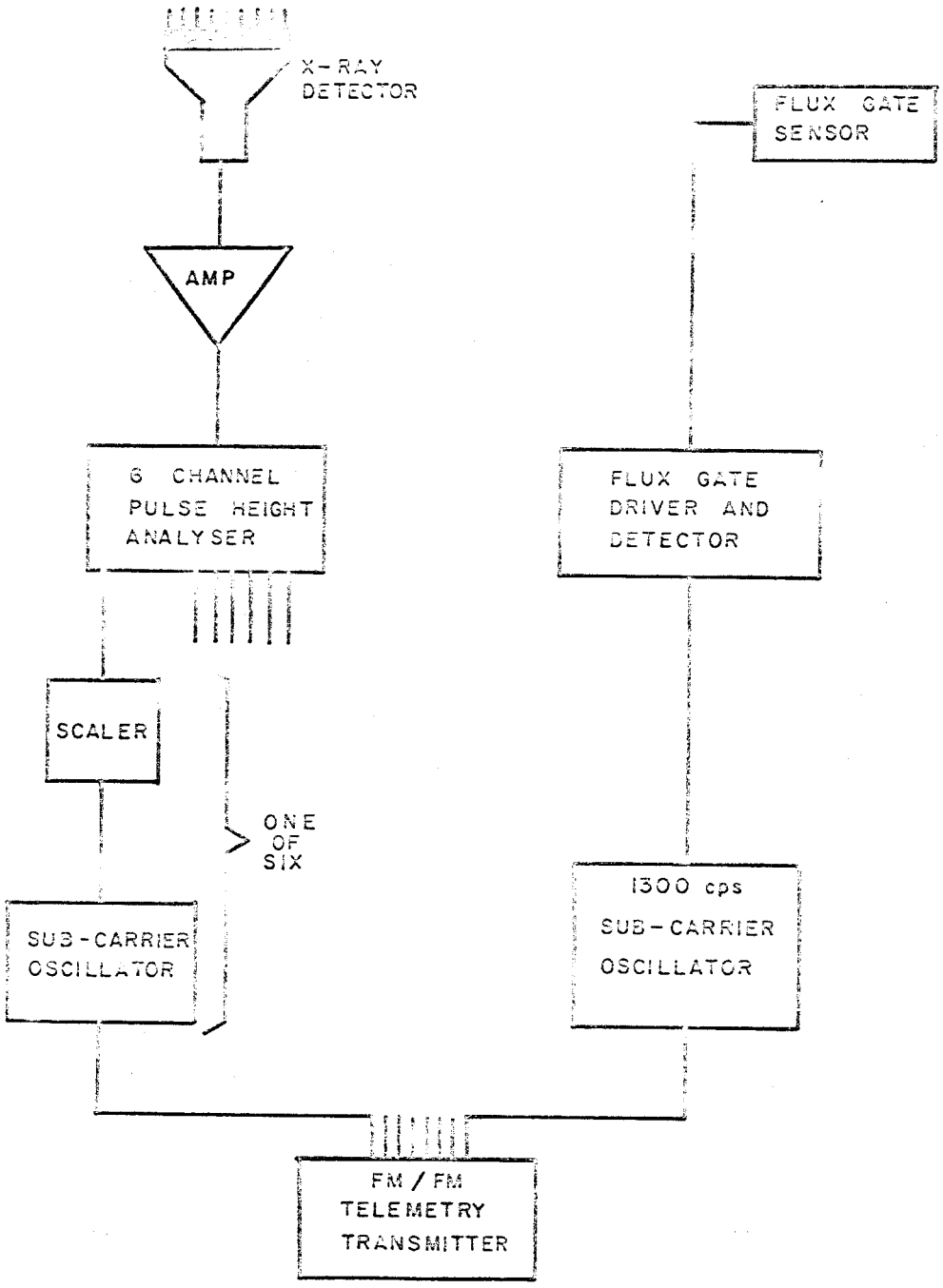

GROUND STATION

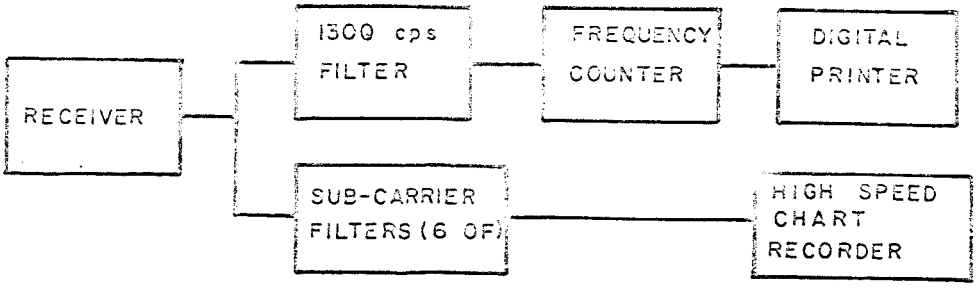

FIG 3

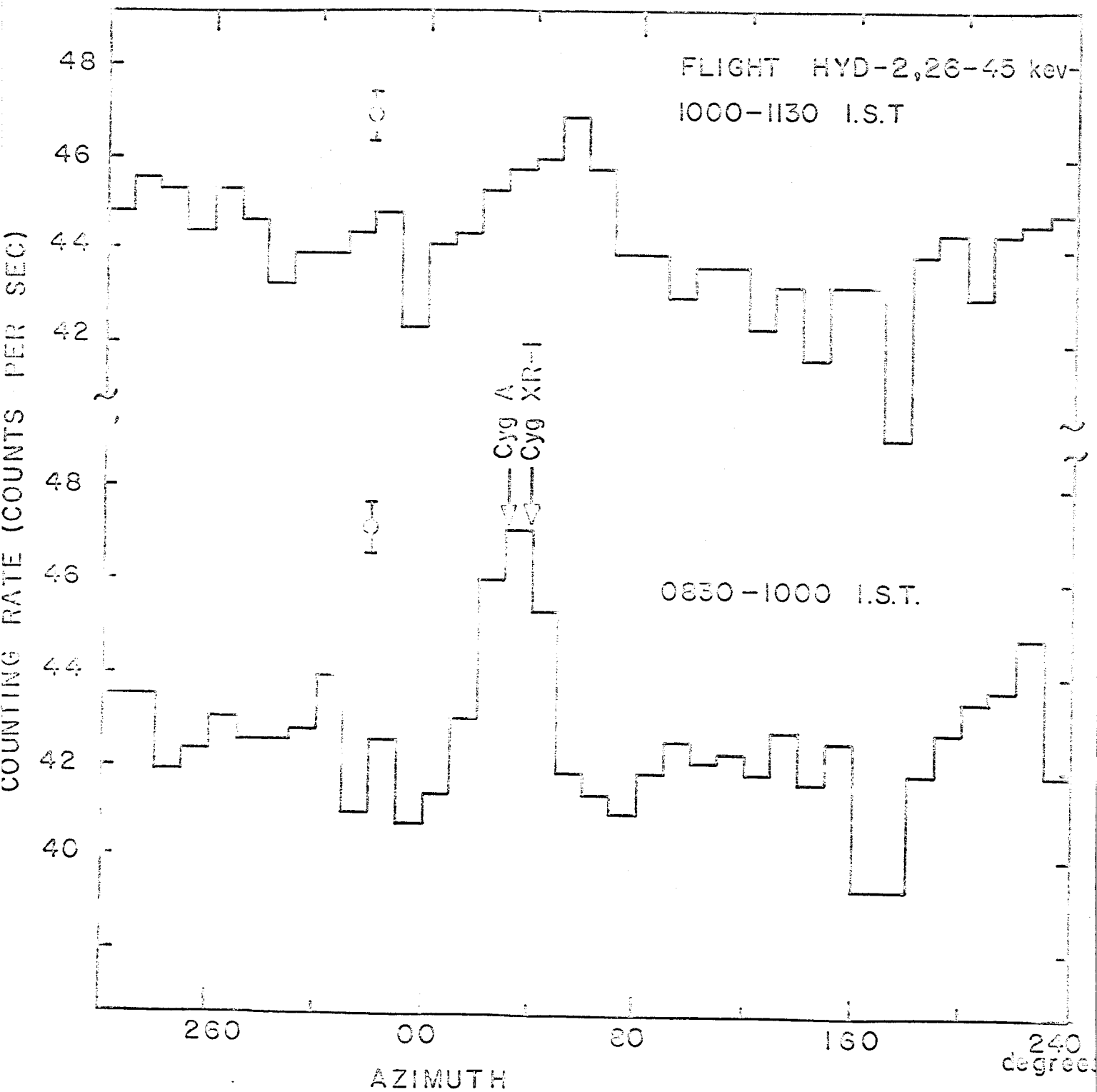
FLIGHT HYD-2,26-45 kev-
1000-1130 I.S.T
0830-1000 I.S.T.
Cyg A
Cyg XR-1
COUNTING RATE (COUNTS PER SEC)
48
46
44
42
40
260
00
80
160
240
degrees
AZIMUTH

FIG. 4

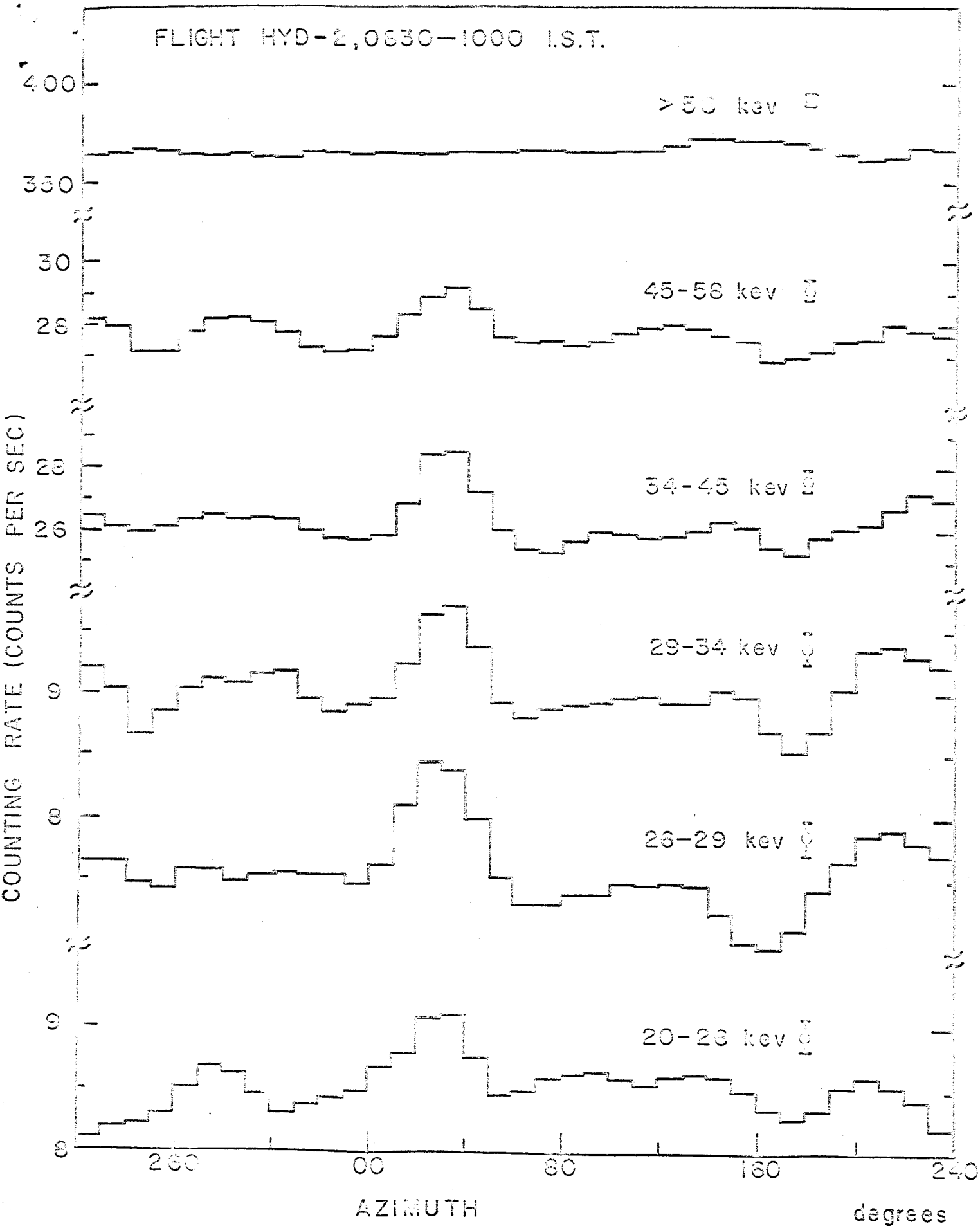
FLIGHT HYD-2,0630-1000 I.S.T.
400
350
>50 kev
30
26
45-58 kev
28
26
34-45 kev
9
29-34 kev
8
26-29 kev
9
8
20-26 kev
COUNTING RATE (COUNTS PER SEC)
260
00
80
160
240
AZIMUTH
degrees

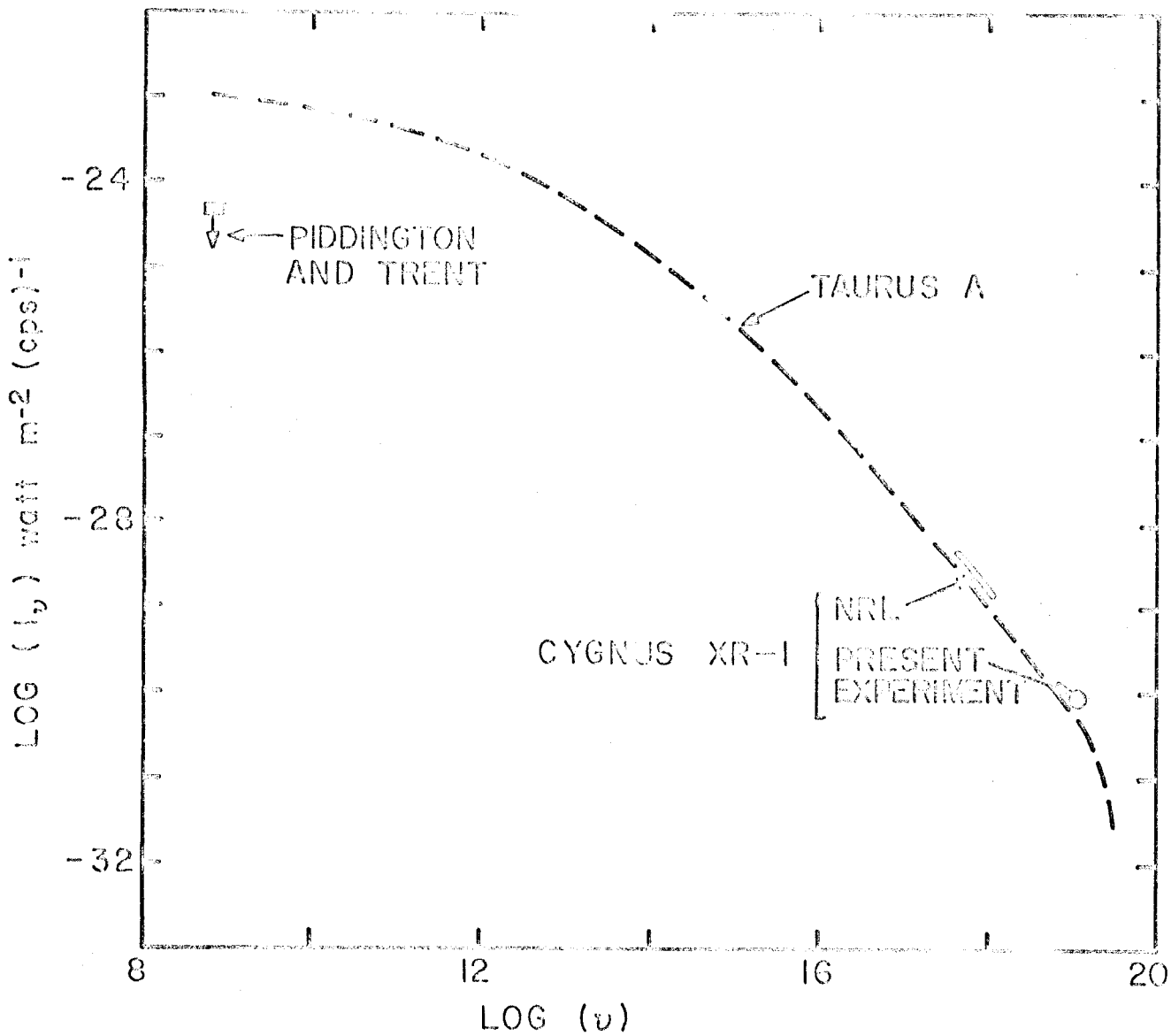
-24
-28
-32
LOG (I_ν) watt m^{-2} (cps)$^{-1}$
8
12
16
20
LOG (ν)
PIDDINGTON
AND TRENT
TAURUS A
CYGNUS XR-1
NRL
PRESENT
EXPERIMENT

FIG. 6